2003

# Intense vortex pinning enhanced by semicrystalline defect traps in self-aligned nanostructured MgB2

S. Li
*Nanyang Technological University, Singapore*

T. White
*Institute of Environmental Science and Engineering, Singapore*

K. Laursen
*Institute of Environmental Science and Engineering, Singapore*

T. T. Tan
*Nanyang Technological University, Singapore*

C. Q. Sun
*Nanyang Technological University, Singapore*

*See next page for additional authors*

# Intense vortex pinning enhanced by semicrystalline defect traps in self-aligned nanostructured $MgB_2$

S. Li[a)]
*School of Materials Engineering, Nanyang Technological University, Singapore 639798*

T. White and K. Laursen
*Center for Advanced Research of Ecomaterials, Institute of Environmental Science and Engineering, Singapore*

T. T. Tan and C. Q. Sun
*School of Materials Engineering, Nanyang Technological University, Singapore 639798*

Z. L. Dong and Y. Li
*Center for Advanced Research of Ecomaterials, Institute of Environmental Science and Engineering, Singapore*

S. H. Zho, J. Horvat, and S. X. Dou
*Institute of Superconducting and Electronic Materials, Wollongong University, NSW 2522, Australia*

(Received 17 March 2003; accepted 21 May 2003)

In this work, we report the discovery of a vortex pinning source: semicrystalline defect wells in self-aligned nanostructured $MgB_2$. It is demonstrated that these aperiodic regions trap numerous crystal defects migrating along nanodomain boundaries during self-alignment and act as intense vortex pinning centers that significantly enhance the high-field performance of $MgB_2$. This suggests that the density of trapped defects in the wells is much greater than that found in other vortex pinning sources. © *2003 American Institute of Physics.* [DOI: 10.1063/1.1591070]

The discovery of superconductivity at 39 K in $MgB_2$ has initiated enormous scientific interest in order to understand and develop this material to better exploit its high intrinsic performance for magnetic and electronic applications.[1,2] It is believed that the supercurrent density in $MgB_2$ is controlled predominantly by flux pinning rather than by the grain boundary connectivity.[3] However, the lack of natural defects is responsible for the rapid decline of critical current density ($J_c$) with increasing field strength.[4] In order to improve the high-field performance of $MgB_2$, a number of techniques have been used to induce crystal defects by atomic displacement, inclusions, grain boundaries, and lattice distortion etc.[5–9] Although a significant flux pinning enhancement in a mixture of $MgB_2$ and SiC has been reported,[10] effective new vortex pinning sources that can further enhance the high-field performance of $MgB_2$ are eagerly awaited. In this work, we report the discovery of a vortex pinning source: semicrystalline defect wells in self-aligned nanostructured $MgB_2$.

$MgB_2$ samples were prepared by pressing a mixture of Mg 99% purity and amorphous B 99% purity powders in the stoichiometeric ratio of Mg:B=1:2 with addition of 10 wt % SiC powder into the pellets. The pellets were sealed in an Fe tube and subsequently sintered at 700–900 °C for 1 h in flowing high purity argon, followed by furnace cooling to produce $MgB_2$ (81.1%) with impurities of MgO (11.36%) and $Mg_2Si$ (7.54%) as determined by quantitative x-ray diffraction (XRD). Magnetization **M** as a function of magnetic field **H** applied along the longitudinal dimension of the sample was measured in a field range of $|\mathbf{H}| \leqslant 9$ T at 20 K using quantum design magnetic property and physical property measurement systems. The field dependence of the critical current density $J_c(H)$ was derived from $M-H$ loops using Bean critical theory. High-resolution transmission electron microscopy (HRTEM) was employed to characterize the morphology of as-sintered samples.

Lattice parameters measured by XRD and refined by the Rietveld method in the as-sintered $MgB_2$ sample with the secondary phases ($Mg_2Si$ and MgO) are $a=3.0856(4)$ Å and $c=3.5296(7)$ Å, a result within experimental error of original commercial $MgB_2$ powder ($a=3.0864$ Å, $c=3.5227$ Å). It indicates that lattice substitution is insignificant in the as-sintered sample. This conclusion is also supported by x-ray photoelectron spectroscopy measurement, which shows no shift in $Mg^{2+}$ binding energy (307 eV) in the polyphase material. Elemental microdistribution mapped by energy-dispersive x-ray spectroscopy shows the MgO and $Mg_2Si$ regions are in micron scale and too large to act as vortex pinning centers.

HRTEM lattice images of $MgB_2$ (211) planes show well-aligned nanodomains with rectangular shapes of $2\sim4$ nm $\times 1$ nm dimension [Fig. 1(a)]. However, alignment is imperfect and a small angle boundary of 2° is discernable in the area marked ''A.'' Such nanostructures were commonly observed in other areas of the sample [Fig. 1(b)] and it dominates the structure of the material. Although the evolution of the structure was not observed *in situ*, the small-angle boundaries around the well-aligned domains suggest a possible formation mechanism of nanostructured $MgB_2$.

It has been reported that $MgB_2$ forms in a process of Mg vapor diffusion into the amorphous B matrix.[11] In this case, the aperiodic arrangement of B atoms in the amorphous

[a)]Author to whom correspondence should be addressed; electronic mail: assxli@ntu.edu.sg

 

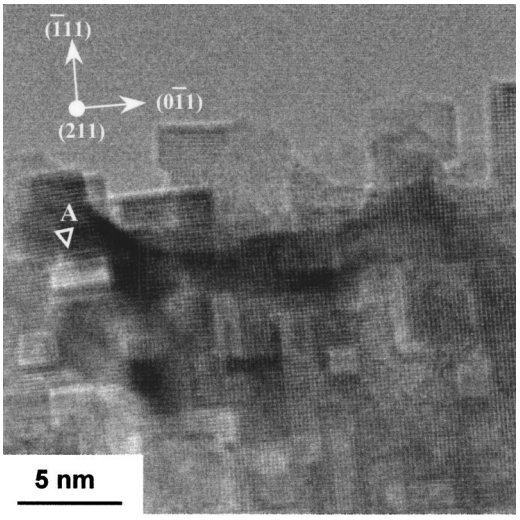


(a)

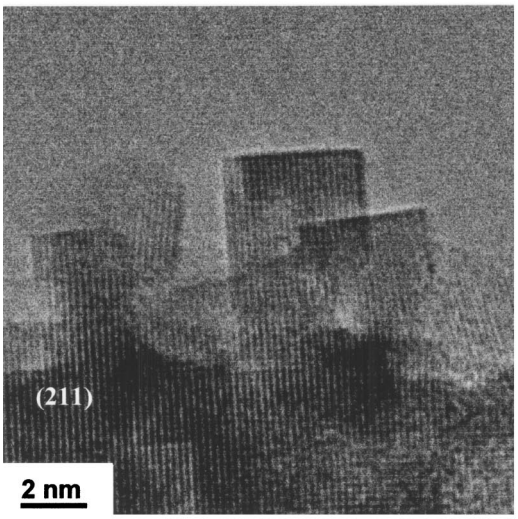


(b)

FIG. 1. (a) HRTEM morphology shows that the majority of the nanodomains with rectangular shapes were aligned along [211] in self-aligned nanostructured $MgB_2$. (b) HRTEM morphology shows similar structure appearing in other areas of the sample.

phase could lead to atomic defects, such as dislocations in the reaction product. During crystallization, dislocation walls will coalesce [Fig. 2(a)]. Stresses at the dislocation wall terminations will combine with surrounding edge dislocations, leading to further wall growth [Fig. 2(b)] and formation of small angle boundaries that connect well-ordered nanodomains [Fig. 2(c)]. To minimize the energy of the system, the dislocations migrate to interdomain boundaries surrounding the nanodomains. These dislocation rearrangements result in rotation of nanodomains A and B to form a contiguous crystal [Fig. 2(d)]. By continuing this subgrain rotation process on neighboring nanodomains [Fig. 2(e)], large (211) nanodomains can be aligned as observed by HRTEM [Fig. 1(a)].

Dislocations in neighboring boundaries can interact in two ways: (1) those of opposite signs from adjacent boundaries will self-compensate and facilitate the further alignment of the nanodomains, while (2) the leading dislocations incorporated from neighboring boundaries, which have the same sign but opposite slip directions, would restrict each other to slide further, obstructing the dislocation incorporating subsequently and thus inhibiting the alignment. In the latter case, there is competition between dislocation incorporation and interaction. From a thermodynamics viewpoint, dislocation incorporation is the favored process when the number of incorporated dislocations is small. Once the number of dislocations piled in front of the leading dislocation, which incorporates from the neighboring boundary, reaches a threshold level, the alignment of the nanodomains in the area would cease, resulting locally in higher lattice energy. This process not only takes place in the horizontal ($X$) dimension but also the vertical dimension ($Y$). When the piled dislocations from two dimensions meet at a point with the arrangement as shown in Fig. 3(a), the strain caused by the piled dislocations can be released. The dislocation arrangement in Fig. 3(a) results in a defect well to trap the dislocations from the boundaries, further aligning the nanodomains. The HRTEM image in Fig. 3(b) shows a square nanowell ($1\times1\ nm^2$) surrounded by periodic crystalline nanodomains. The near-atomic resolution detail within the nanowell is consistent with aperiodic structure and provides direct evidence for the formation of a semicrystalline defect trap in the self-aligned

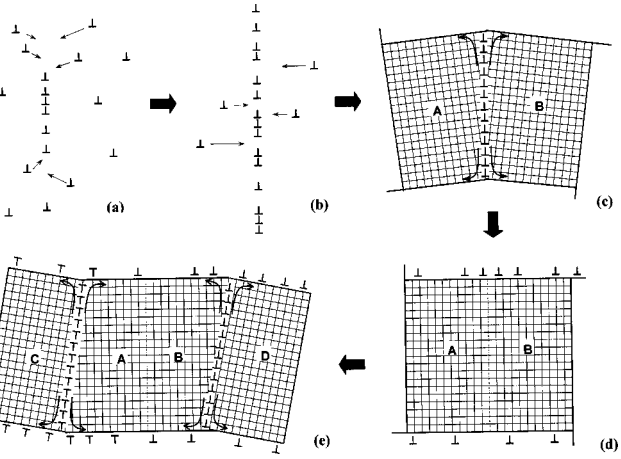


FIG. 2. A schematic illustration showing (a) a random array of dislocations forming in the processing of the diffusion of Mg vapor in the amorphous **B** matrix, (b) stress at the end of a dislocation wall segment attracting surrounding edge dislocations resulting in wall growth, (c) small angle boundary formation of nanodomains, (d) dislocation rearrangements resulting in a rotation of nanodomains and the dislocation piling in the boundaries after self-alignment, and (e) piled dislocation arrangements from adjacent nanodomains in the horizontal dimension during the self-alignment processing.

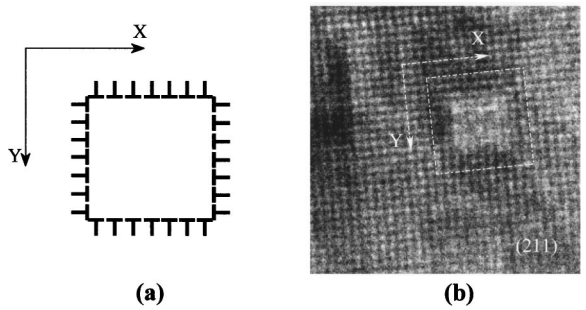


FIG. 3. (a) Schematic of defect well formed through the meeting of dislocations at a point. (b) Direct observation of a nanodefect well by HRTEM. Note the nanodefect well has semicrystalline structure.

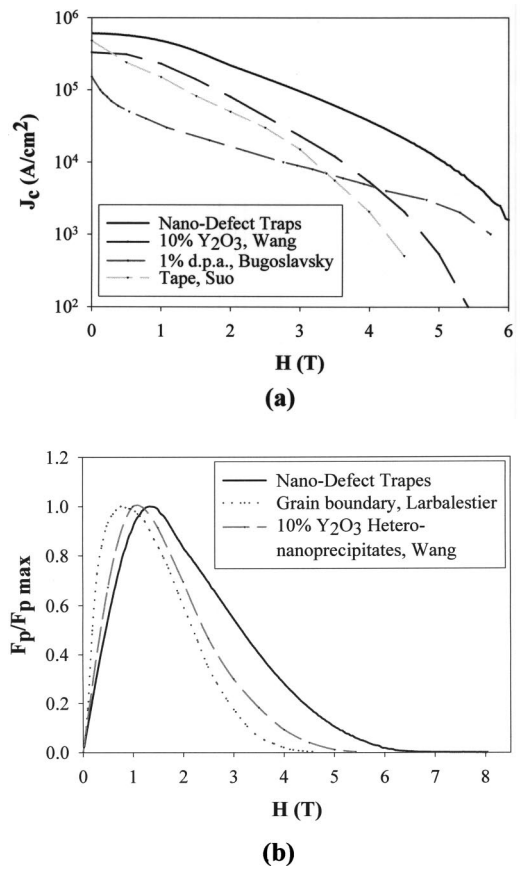


FIG. 4. (a) The magnetic $J_c(H)$ for $MgB_2$ with nanodefect traps at 20 K compared with the data reported for other vortex pinning sources. (b) The field dependence of flux pinning force density shows that the pinning force density of the defect traps is much greater than other vortex pinning sources, such as grain boundaries and heteronanoparticles.

nanostructured $MgB_2$. However, defect traps can only release local strain. On a large scale, many similar semicrystalline defect traps are formed and dispersed throughout the material, as shown in Fig. 1(a). It is believed that the addition of SiC in $MgB_2$ facilitates the formation of self-aligned nanostructured $MgB_2$ through promotion of incipient melting, but the nature of facilitation is still under investigation.

Nonetheless, whatever the mechanism of formation, it is clear that nanodefect traps substantially enhance the high field performance of $MgB_2$. Figure 4(a) compares the magnetic $J_c(H)$ for material having nanodefect traps at 20 K with literature data. It can be seen that the sample with nanodefect traps has high $J_c$ as well as excellent field performance, particularly in high field. These superior properties indicate that the pinning force of the semicrystalline defect trap is much greater than that of the other vortex pinning sources. The flux pinning enhancement of the semicrystalline nanodefect trap is also demonstrated by the field dependence of flux pinning force density as shown in Fig. 4(b), which compares the pinning force density of the nanodefect traps with the reported data of the other pinning sources in bulk materials. The dotted line presents the field dependence at 20 K of the relative pinning force density measured from a sample in which the supercurrent density is mostly determined by the flux pinning of grain boundaries. It shows that the flux-pinning force density curve, as the function of the applied field, matches the curve contributed purely by the pinning of grain boundaries.[3] In the sample doped with heteronanoprecipitates ($Y_2O_3$), the maximum pinning force density shifts toward higher field, and reveals that vortex pinning is not only augmented by grain boundaries, but also by inclusions. However, the field dependence of the pinning force density [solid line in Fig. 4(b)], measured from the sample with nanodefect traps, is much greater than that observed in those samples in which pinning is enhanced only by grain boundaries and inclusions. The maximum pinning force density is increased to 1.34 from 0.76 T for pinning by grain boundaries. The volume pinning force density of 5.5 GN/m$^3$ at 20 K is comparable to that of NbTi at 4.2 K. This indicates that the density of the trapped defects in the semicrystalline nanodefect wells is an order of magnitude greater than that found in other vortex pinning sources. However, similar $J_c(0)$ in all samples [Fig. 4(a)] suggests that the highly aligned nanostructure of the present sample does not greatly contribute to the critical current density in zero field, supporting the notion that the $MgB_2$ is not compromised by a weak-link problem.[2,3]

In summary, the significant enhancement of flux pinning in the high-field performance of $MgB_2$ reveals the formation of a vortex pinning source: semicrystalline nanodefect traps in self-aligned nanostructured $MgB_2$. It is observed that the [211] zone is the favored orientation for crystal growth and it suggests that the (211) plane may have lower surface energy of the system. Dislocation incorporation from small-angle domain boundaries results in large-scale alignment of the nanodomains in three dimensions. When orthogonal dislocations of different signs meet at a point in the (211) plane, nanodefect wells are formed to release the strain caused by the rotations of nanodomains. Such wells trap numerous crystal defects from the boundaries to act as the vortex pinning centers with intense pinning force, thus enhancing the high-field performance of $MgB_2$ significantly.

[1] J. Nagamatsu, N. Nakagawa, T. Muranaka, Y. Zenitani, and J. Akimitsu, Nature (London) **410**, 63 (2001).
[2] D. Larbalestier, A. Gurevich, D. M. Feldmann, and A. Polyanskii, Nature (London) **414**, 368 (2001).
[3] D. C. Larbalestier, L. D. Cooley, M. O. Rikel, A. A. Polyanskil, J. Jiang, S. Patnalk, X. Y. Cai, D. M. Feldmann, A. Gurevich, A. A. Squitieri, M. T. Naus, C. B. Eom, E. E. Hellstrom, R. J. Cava, K. A. Regan, N. Rogado, M. A. Hayward, T. He, J. S. Slusky, K. Khalifah, K. Inumaru, and M. Haas, Nature (London) **410**, 186 (2001).
[4] Y. Bugoslavsky, G. K. Perkins, X. Qi, L. F. Cohen, and A. D. Caplin, Nature (London) **410**, 563 (2001).
[5] Y. Bugoslavsky, L. F. Cohen, G. K. Perkins, M. Pollchetti, T. J. Tate, R. Gwilliam, and A. D. Caplin, Nature (London) **411**, 561 (2001).
[6] C. B. Eom, M. K. Lee, J. H. Chol, L. J. Belenky, X. Song, L. D. Cooley, M. T. Naus, S. Patanik, J. Jiang, M. Rikei, A. Polyanski, A. Gurevich, X. Y. Cai, S. D. Bu, S. E. Babcock, E. E. Hellstrom, D. C. Larbalestier, N. Rogado, K. A. Regan, M. A. Hayward, T. He, J. S. Slusky, K. Inumaru, M. K. Haas, and R. J. Cava, Nature (London) **411**, 558 (2001).
[7] X. Z. Liao, A. C. Erquis, Y. T. Zhu, J. Y. Huang, D. E. Peterson, F. M. Mueller, and H. F. Xu, Appl. Phys. Lett. **80**, 4398 (2002).
[8] J. Wang, Y. Bugoslavsky, A. Berenov, L. Cowey, A. D. Caplin, L. F. Cohen, L. D. Cooley, X. Song, and D. C. Larbalestier, Appl. Phys. Lett. **81**, 2026 (2002).
[9] H. L. Suo, C. Beneduce, X. D. Su, and R. Flükiger, Supercond. Sci. Technol. **15**, 1058 (2002).
[10] S. X. Dou, S. Soltanian, J. Horvat, X. L. Wang, S. H. Zhou, M. Ionescu, H. K. Liu, P. Munroe, and M. Tomsic, Appl. Phys. Lett. **81**, 3419 (2002).
[11] P. C. Canfield, D. K. Finnemore, S. L. Bud'ko, J. E. Ostenson, G. Lapertot, C. E. Cunningham, and C. Petrovic, Phys. Rev. Lett. **86**, 2423 (2001).